inner satellites are a secondary population, re-accumulated out of debris of the first generation destroyed by Triton's passages.

Pluto-Charon system.– Because of its distance and the lack of flyby observations, this is the least known satellite system. Very little is known about Pluto and Charon's composition and internal structure. Their comparable masses ($\simeq 1.3 \times 10^{25}$ g against $\simeq 1.5 \times 10^{24}$ g) suggest an unusual origin, perhaps a giant impact like that for the Moon. Their tidal influence (Pluto on Charon and vice versa) is also comparable and large ($\approx 10^{-4}$); this suggests that the present, doubly synchronous state, in which both rotational periods are equal to the orbital period of 6.39 d, has been attained very quickly, perhaps in 10 – 100 My. Perturbations in the system may be produced by encounters with comets from the transneptunian region, but should quickly damp out. Recent Hubble Space Telescope and ground-based adaptive optics observations indicate an anomalous eccentricity $\lesssim 0.0075$ for this system, perhaps an indication of a recent impact on one of the two bodies; however, this result is debated.

14.3 Asteroids

Among the observed members of the solar system, asteroids represent by far the most numerous population. The number of catalogued bodies is now greater than 3×10^5 (of which $\approx 50,000$ have very precisely determined orbits and have been given a catalogue number); $\approx 95\%$ of them orbit around the Sun in moderately eccentric and inclined orbits in a large toroidal region between 2.1 and 3.3 AU, the *main asteroid belt*. In this belt the accretion of a planet-size object was interrupted in the early stage of the solar system evolution, leaving the asteroid population. The orbital and physical parameters of the ten largest asteroids are listed in the Table 14.5. Moreover, some $5,000$ asteroids – called planet-crossing – are known, with perihelia inside the orbits of the inner planets. The best characterized is the population of *near-Earth asteroids* (with about $1,600$ known objects), which occasionally approach the Earth; this allows precise optical and radar observations. Their possible collision with the Earth makes them a potential hazard. Beyond the main belt, near Jupiter's triangular Lagrangian points (Sec. 13.3), there are the two groups of *Trojan and Greek asteroids*.

Orbital structures in the main belt. Understanding the orbital dynamics in the asteroid belt is not straightforward, because Jupiter and Saturn cause significant variations in most orbital elements. For instance, typical variations in eccentricity and inclination may be of order $\approx 0.1 - 0.3$ and $\approx 5^\circ - 10^\circ$ respectively, with timescales ranging from years to hundreds of millennia. Thus it is necessary to first subtract these perturbations. The outcome of this delicate correction, performed at different levels of sophistication either analytically or numerically, are the so called *proper orbital elements* (Sec. 15.1). Except in resonances, the angular variables undergo a steady circulation, so that only

Table 14.5. Orbital and physical parameters of the ten largest asteroids: (a, e, I) are proper orbital elements (from http://newton.dm.unipi.it), D is the mean size estimated with infrared observations of the IRAS spacecraft, P the spin period and LV the range of variation of the light curve (from http://cfa-www.harvard.edu/iau/lists/LightcurveDat.htm). For a triaxial ellipsoid, assuming that the brightness is proportional to the cross-section as seen from the Earth (uniform albedo approximation), the light-curve variation gives an indication of the ratios of the principal axes.

No.	Name	a (AU)	e	I (deg)	D (km)⋆	P (h)	LV (mag)
1	Ceres	2.767	0.116	9.66	848.4	9.075	0.04
2	Pallas	2.771	0.281	33.20	498.1	7.811	0.03-0.16
4	Vesta	2.362	0.099	6.39	468.3	5.342	0.12
10	Hygiea	3.142	0.136	5.10	407.1	27.623	0.11-0.33
511	Davida	3.174	0.190	14.25	326.1	5.129	0.06-0.25
704	Interamnia	3.061	0.104	18.79	316.6	8.727	0.03-0.11
52	Europa	3.097	0.119	6.37	302.5	5.633	0.09-0.20
87	Sylvia	3.485	0.054	9.85	260.9	5.184	0.30-0.62
31	Euphrosyne	3.155	0.208	26.54	255.9	5.531	0.09-0.13
15	Eunomia	2.644	0.149	13.10	255.3	6.083	0.40-0.56

⋆ The IRAS sizes are likely underestimates; more precise observations by the ISO spacecraft yield 959.2 km, 574.0 km and 578.0 km for the major axes of Ceres, Pallas and Vesta, respectively.

semimajor axis, eccentricity and inclination acquire proper values. The proper elements are never ideal orbital constants, but their validity is limited to some time interval. Typically, a stability over $\approx$ My is attained, but attempting to stretch this limit to hundreds of My or Gy, still shorter than the age of the solar system, is dangerous. Tiny details of gravitational perturbations due to the planets may cause instability (e.g., effects related to high-order resonances; Sec. 12.5); also some non-gravitational forces may cause orbital changes for asteroids smaller than $\approx$ 20 km in size (e.g., the Yarkovsky effect; Sec. 15.4).

Figure 14.3 shows the distribution of the proper elements in the main asteroid belt. Within the estimated stability interval of $\approx$ 10 My, each point represents a single asteroid. A closer look indicates the major structural features, of dynamical and collisional origin: (i) paucity of asteroids in the mean motion and secular resonances with the planets; (ii) several distinct groupings of the proper elements throughout the whole belt; and (iii) truncation of the belt at the encounter threshold with Mars (perihelion $\simeq$ 1.66 AU). The large mean values of the proper eccentricity and inclination ($\overline{e} \simeq 0.13$ and $\overline{I} \simeq 7^\circ$ respectively) do not fit the simplest expectation of a disc with objects on primordial orbits with low eccentricity and inclination. Apparently some process "excited" their orbits since the asteroids accreted in this zone some 4.5 Gy ago. The acquired mean velocity can be estimated as $\approx \frac{1}{2} na \sqrt{\overline{e}^2 + I^2} \simeq 1.7$ km/s

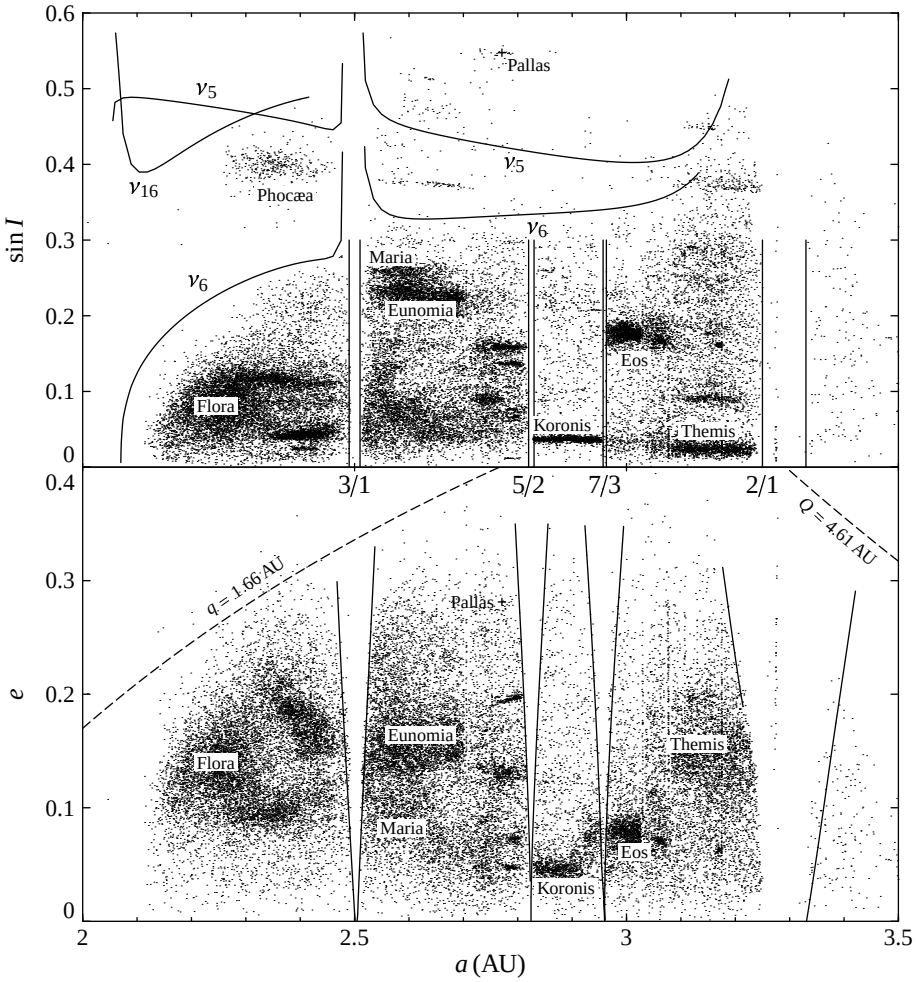

Figure 14.3. Proper orbital elements of the main-belt asteroids in the $(a, \sin I)$ (top) and (a, e) planes; on the bottom, q and Q are, respectively, the perihelion and aphelion distances. The main belt is delimited by the ν_6 resonance at the bottom ($a \simeq 2.1$ AU), and the $2/1$ mean motion resonance with Jupiter on top ($a \simeq 3.25$ AU). There are other mean motion resonances ($3/1$, $5/2$, etc.) associated with the paucity of asteroids due to the fast chaotic evolution towards very eccentric states (Kirkwood gaps); solid lines indicate the borders of the corresponding resonances. Unstable orbits with large inclinations are due to the ν_5 and ν_{16} resonances (Sec. 15.1), so that only a small stable island is populated by the Phocæas. On the other hand, the first order mean motion resonances with Jupiter – 2/1, 3/2, 4/3 – harbour small populations of stable orbits. A number of asteroids are clustered in families, of which the most significant ones are labelled. More than $35,000$ asteroids have been included, which are numbered or have been observed in more than one opposition; data from http://newton.dm.unipi.it/.

(n is the mean motion and $a \simeq 2.5$ AU), while the mean relative velocity is $\simeq 5$ km/s; this is approximately 4 times higher than the escape velocity of the largest asteroid, Ceres, and causes disruptive collisions, rather than accumulation. Moreover, the estimated total mass in the main belt – about $5 \times 10^{-4}\, M_\oplus$ – is two or three orders of magnitude below the mass estimated in this zone from a smooth distribution of the surface density in the primordial planetary nebula (Fig. 16.1). This again gives a hint into the "violent history" in this zone of the solar system.

Dynamical features in the main asteroid belt: resonances.– Resonances with the major planets sculpt both the borders of the main asteroid belt and the regions inside; at their locations a significant paucity of asteroids is observed. These empty regions – *Kirkwood gaps* – in the asteroid distribution were noticed by D. Kirkwood as early as in the middle 19th century. The most prominent of them are associated with low order, mean motion commensurabilities, like 3/1 or 5/2, with Jupiter. As noted in Sec. 12.5, higher-order resonances are less significant; however, what matters is their structure. Resonance dynamics in the main asteroid belt has been understood in detail only with the help of advanced analytic techniques and extensive numerical experiments. It was found, for instance, that the 3/1 mean motion commensurability with Jupiter at ≈ 2.5 AU is highly unstable, due to secular resonances located inside its phase space region. Objects injected in this region quickly (in $\approx$ My) increase their eccentricity to very high values (close to unity) by collisions, or slow diffusion due to the Yarkovsky effect. As a consequence, typically they eventually fall into the Sun, unless they are released from the resonance by a close encounter with one of the inner planets, or with Jupiter (in $\approx 5\%$ of the cases); then the asteroid becomes a member of the planet-crossing population. On the other hand, the first-order (2/1, 3/2, 4/3) mean motion resonances with Jupiter harbour limited stable regions where asteroids may reside for $\approx$ Gy; they are called Zhongguo group (2/1), Hilda group (3/2) and Thule group (4/3). The large populations of Trojans and Greeks (Sec. 13.3) are also in the 1/1 resonance with Jupiter.

The second kind of resonances significant for asteroidal motion are the secular ones; they occur when the mean drift of the pericentre or the node becomes commensurable with one of the proper frequencies of the planetary system (Sec. 15.1). The most significant one – called ν_6 – appears when the longitude of the pericentre ϖ drifts, due to planetary perturbations[2], at the rate $g_6 \simeq 28.2''$/y. This resonance truncates the belt at ≈ 2.1 AU and also causes the "bent" boundary in the (a, I) plane (Fig. 14.3). As in the 3/1 case, asteroidal

[2]It is often inaccurately stated that this is a resonance with Saturn's pericentre drift; the principal perturbing effect, however, arises due to Jupiter, which pericentre is also largely affected, but not dominated, by this frequency; see Fig. 15.1b.

orbits injected in its zone evolve on a ≈ My timescale toward a very eccentric state where they either are released from the resonance due to a close encounter with an inner planet, or collide with the Sun.

Collisional and Yarkovsky-driven injection mechanisms resupply objects in the 3/1, 5/2 and ν_6 resonances at a rate far too low to compensate the fast eccentricity evolution. This is the reason why we see only a few objects *inside* their phase space region. In spite of this, the injection rate seems enough to keep the population of planet-crossing asteroids in an approximate steady state. The higher-order, and thus weaker, resonances also produce long-term instabilities by increasing the eccentricity. In these cases, however, the timescale is much longer (e.g., ≈ 0.1 Gy for cases like 7/3, 9/4 etc.), which allows evolution processes strong enough to resupply asteroids (and meteoroids); no significant void in their distribution is observed. Note also that their widths (depending on the order) are small as well. On the whole, resonant effects cause a permanent leakage of asteroids from the main belt, important for understanding their populations on planet-crossing orbits.

Collisional features in the main asteroid belt: asteroid families.– As discovered in 1918 by K. Hirayama, the orbital parameters of asteroids indicate prominent groupings in the space of proper elements. Hirayama suggested that the origin of each of these *asteroid families* could be traced back to the collisional breakup of a parent body, which ejected fragments into heliocentric orbits with relative velocities much lower than their orbital speed. An increasing number of precisely known asteroidal orbits have allowed us to identify some 40 families across the whole main belt; families may also exist among the Trojans and even in the transneptunian region. They are usually named after the largest member.

Physical studies have shown that the members of the most populous families (associated with Themis, Eos, Koronis and Vesta) have similar surface compositions, supporting the hypothesis of a common origin. It also opened up the possibility of investigating directly by astronomical observations the interior structure of the parent bodies; this has been accomplished, in fact, after recent discovery of a very young asteroid cluster inside the Koronis family (Fig. 14.4), named after its biggest member the *Karin cluster*; it has been interpreted as an output of a collisional disruption of ≃ 25 km size parent body occurred only some 5.8 My ago. Because of its very young age, the Karin cluster has undergone little dynamical and collisional evolution, and is thus ideal to investigate physical processes in collisions of small asteroids. Several other tight asteroidal clusters of collisional origin have been recently discovered.

Collisional fragmentation has been shown to be a plausible formation process for families, from the point of view of the collision probability. Studies of size distribution of families members indicate that at least the most prominent of them are 1 – 3 Gy old (except for the Karin cluster, whose age is known

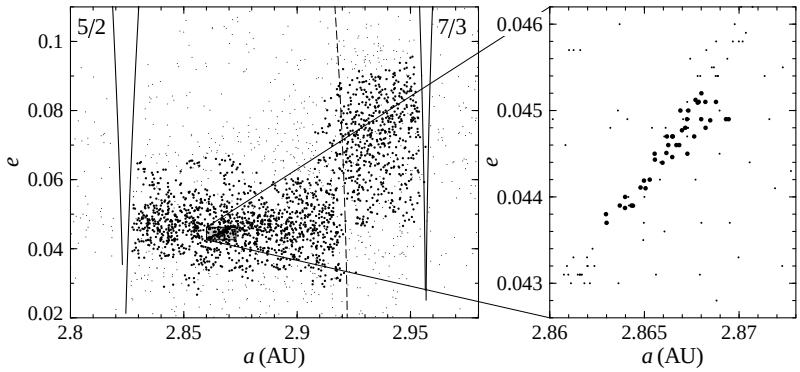

Figure 14.4. The Koronis asteroid family (thick dots on the left) on the plane (a, e); background asteroids, not associated with the family, are shown by thin dots. Note the sharp truncation of the family by the 5/2 and 7/3 mean motion resonances with Jupiter; the offset in proper eccentricity at larger values of the proper semimajor axis ("Prometheus group") is due to an interaction with a weak secular resonance (dashed line). A recent secondary break up of a member of this family with size $\simeq$ 25 km has created the Karin cluster (right); for comparison, the estimated size of the Koronis parent body is $\simeq$ 120 km. Proper elements from http://newton.dm.unipi.it/; see also W.F. Bottke et al., *Science* **294**, 1693 (2001) and D. Nesvorný et al., *Nature* **417**, 720 (2002).

much more precisely). They also suggest a wide variety of collisional modes: from the entire disruption of the target body by a projectile of comparable mass (e.g., the case of Koronis family), to a family composed of a swarm of small asteroids, probably all ejecta from a large target hit by a small projectile (e.g., the Vesta family). Asteroidal collisions have been simulated in laboratory experiments with high-velocity impacts on solid targets, and on computers using very sophisticated numerical programs. It has been thus verified that most energetic collisions are disruptive simply because the relative velocities of asteroids, due to their eccentricities and inclinations, largely exceed their escape velocities; even impacts with projectile-to-target mass ratios $\approx 0.1\%$ can impart energies exceeding the binding energy of the target bodies. The large estimated age of the principal families and the short-term validity of proper elements imply that they might have undergone dynamical evolution. It is likely that families were initially represented in the space of proper elements by more compact clusters and then expanded, due to long-term perturbations, such as high-order resonances and the Yarkovsky effect (this latter for sizes $\leq$ 20 km). This kind of dynamical aging, aside from collisional grinding, also explains why many asteroid families are sharply truncated by the strongest resonances in the main asteroid belt (Fig. 14.4). There is another important consequence of this scenario: asteroid families and the entire main asteroid belt, though Gys old, may still be very efficient in delivering multi-kilometre asteroids to the principal

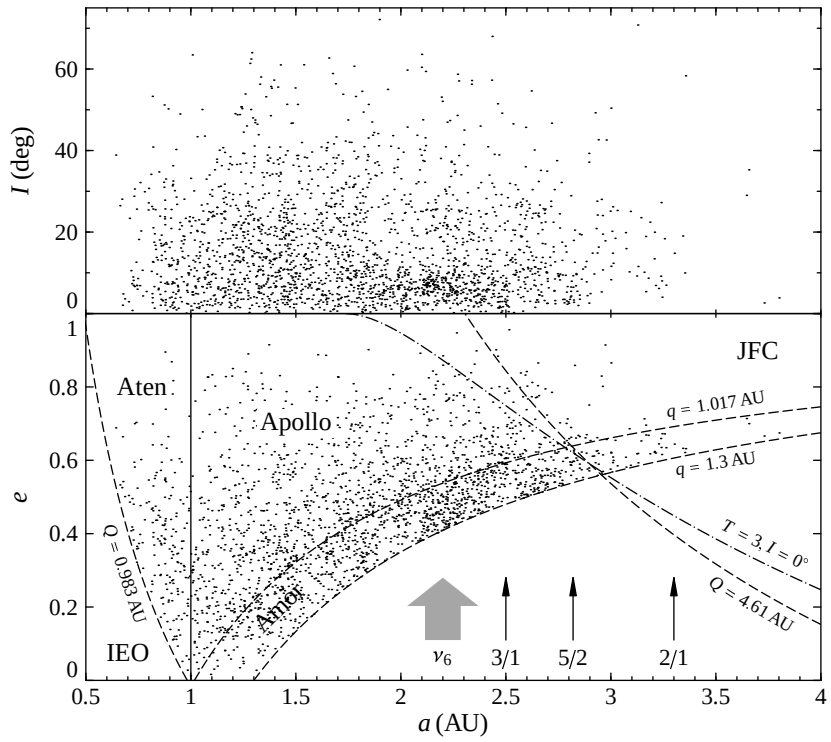

Figure 14.5. Keplerian orbital elements of near-Earth objects ($q \leq 1.3$ AU and $Q \geq 0.983$) in the (a, e) and (a, I) planes. Apollos and Atens are on Earth-crossing orbits; Amors are on near-Earth-crossing orbits (most of them will cross the Earth orbit within next $\approx 10^4$-10^5 y); orbits entirely inside the Earth orbit – (IEO) with $Q < 0.983$ AU – have not yet been detected so far due to strong observational bias. Objects on Jupiter-crossing orbits have $Q \leq 4.61$ AU (long-term minimum perihelion distance of Jupiter), approximately coincide with those having the Tisserand parameter $T = 3$ for zero inclination (see Sec. 14.5). Location of the Jupiter family comets is indicated by JFC. Data of more than 1,600 asteroids from http://newton.dm.unipi.it/.

resonances in the belt (such as the mean motion commensurabilities 3/1 and 5/2 with Jupiter or the ν_6 secular resonance), allowing them to maintain an approximately constant number of the near-Earth asteroids.

"Heating" the main belt. The large mean values of eccentricity and inclination, and a significant mass-loss in the main asteroid belt, require particularly strong perturbations, possibly acting during the early stages of its evolution; a similar problem is encountered when explaining orbital structures in the transneptunian region (Sec. 14.4). The depletion of the primordial main belt may be produced by a combination of two processes: (i) *sweeping mean motion resonances* with Jupiter, and (ii) the *scattering action of massive planetesimals*, later ejected from the solar system by planetary perturbations.

The first mechanism relies on the fact that early Jupiter and Saturn likely changed their distances from the Sun by about a fraction of an AU due to scattering of planetesimals (Sec. 16.4). While Jupiter migrated inward, the mean motion resonances followed and affected a much larger portion of the belt. An alternative model assumes that initially a cluster of cores of similar mass formed in the Jupiter zone and resonantly affected a much larger region before they collapsed to form the planet. This mechanism explains the current paucity of asteroids with $a \geq 3.3$ AU, including the limited population inside first-order resonances, protected from close encounters with Jupiter; but it fails to explain the $\approx 99\%$ mass loss from the original belt.

The second scenario relies on the existence of large planetesimals (of Moon-to-Mars size), a left over of planetary formation in the early asteroid belt or the result of injection by Jupiter's perturbations. If they happened to remain in this region for $\approx 10 - 50$ My, before being ejected out of the solar system by Jupiter's influence, they might have easily excited the eccentricity and inclination of the remaining population to the observed values. This may also explain the very peculiar orbit of Pallas, the second largest asteroid, with $e \simeq 0.28$ and $I \simeq 33.2°$, and the significant mass depletion in the belt zone. Giant collisions may also explain existence of a few large metallic asteroids, including Psyche, $\simeq 260$ km across, which could be remnant cores of large, differentiated primordial objects, stripped of their mantle.

Near-Earth objects. By convention, the near-Earth objects (NEOs) are those with perihelion $q \leq 1.3$ AU and aphelion $Q \geq 0.983$ AU. Traditional groups of this population include the *Apollos* ($a \geq 1$ AU and $q \leq 1.0167$ AU) and *Atens* ($a < 1$ AU and $Q \geq 0.983$ AU); currently both cross the Earth orbit (and may hit the Earth at their node; note that its eccentricity is $\simeq 0.0167$). These two groups are called Earth-crossing objects (ECOs). *Amor* objects are those with $1.0167 < q \leq 1.3$ AU; they can currently approach the Earth orbit, but not collide with it. However, eccentricity variations produced by planetary perturbation may allow Amors to become Apollos for some limited time, of order $10^3 - 10^5$ y. Figure 14.5 summarizes the orbital classes of NEOs. The largest NEOs are currently in the Amor population: Ganymede, ≈ 38.5 km across, Eros and Don Quixote[3], both with sizes of ≈ 20 km. Among ECOs, Ivar and Betulia are the largest bodies, ≈ 8 km across. The smallest known members of the NEO population are a few metres big, aside from the meteorites and dust particles discussed in Sec. 14.6.

A typical dynamical lifetime of a NEO orbit is ≈ 10 My; on a longer timescale the bodies either collide with a terrestrial planet or the Sun, or are

[3]Due to its dust trail, this object is suspected to be a comet remnant. The name near-Earth objects, rather than asteroids, is adopted because part of them may be of cometary origin. The most updated models, however, indicate that comets contribute to the population by less than 10% (for those with $a < 7.4$ AU).

ejected out of the solar system. Thus the NEO population must be continuously replenished to keep an approximate steady state, witnessed by a roughly constant flux of impacting bodies on the lunar surface over the last ≈ 3 Gy. Fast computers and sophisticated integration codes allowed during the past decade major advances in understanding this delicate problem. The main asteroid belt – the nearest vast reservoir – appears to be the dominant source of NEOs with $a < 7.4$ AU via a two-step process: (i) collisional or Yarkovsky-driven injection into the powerful 3/1 and ν_6 resonances, and the subsequent evolution into the planet-crossing zone; and (ii) slow leakage of asteroids into a Mars-crossing (but not NEO) population via weak resonances in the inner part of the main belt (mainly high-order and multiple commensurabilities with giant planets or exterior resonances with Mars), and subsequent evolution into the NEO region by encounters with Mars. These sources altogether account for some $\approx 80 - 90\%$ of NEOs; asteroids in the outer part of the main belt contribute by $\simeq 8\%$. Comets – for a long time a favoured source – contribute the remaining part.

A specific problem of the ECO population is the collision risk with the Earth and evaluation of the related danger for mankind. Sophisticated automated programmes to survey the NEO population and determine the orbit of the *potentially hazardous objects* (PHO) have been set up. In the current definition a PHO has an absolute magnitude (see Useful physical quantities) smaller than 22 (roughly objects larger than 200 m) and the largest distance between its orbit and the Earth's orbit is 0.05 AU. To find the impact hazard, two procedures are usually adopted: (i) further observations and more accurate orbit determination until the risk is found inexistent; or (ii) if the object is too faint, *virtual impactors* are investigated. The orbit of a PHO has an uncertainty which determines a tube around its mean; in the set of all possible orbits, those that correspond to objects which will in fact impact the Earth are computed, and the time at which they will be again observable assessed. In a worldwide effort, observations are carried out; if subsequent tracking of one of such virtual impactor does not confirm its existence, the corresponding risk is set aside.

Obviously, one is mostly interested in hazardous objects a kilometre across or larger. Only $\approx 50 - 60\%$ of them are presently known (of which none is a potential impacting body over next century or so). The unknown part of the kilometre-size NEO population resides on highly eccentric and inclined orbits that are very difficult to observe; nevertheless, the current observation programmes by about 2014 should determine 90% of this population (new ground-based projects, like PanSTARRS, may reach this completion limit even earlier); but this fraction drastically decreases for smaller objects.

Size distribution and collisions of asteroids. Collisional evolution has also substantially affected the mass (and size) distribution of asteroids. The largest

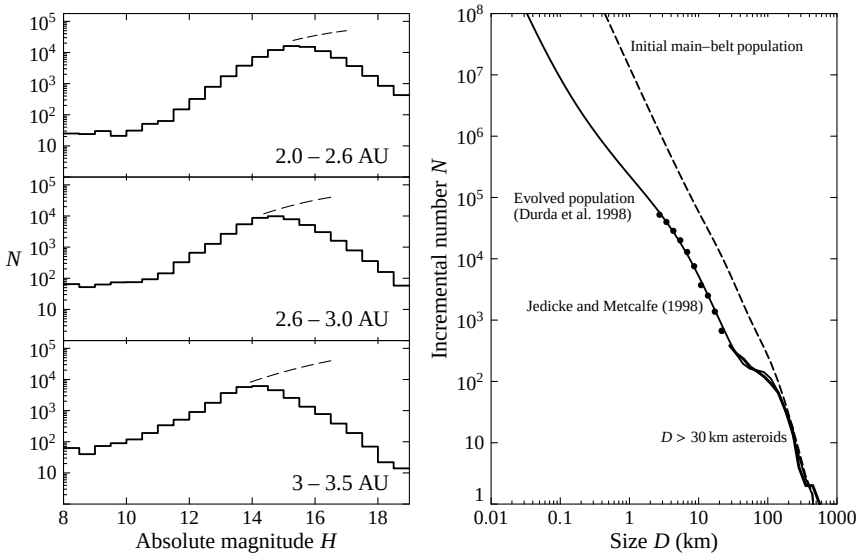

Figure 14.6. Left: number of asteroids in half-magnitude bins vs their absolute magnitude H for three zones in the main asteroid belt. The observed population given by the histogram; the true population is approximated by the dashed lines (the difference is due to observational limitations). Adapted from R. Jedicke and T.S. Metcalfe, *Icarus* **131**, 245 (1998), with updates. Right: the incremental (number of asteroids with size less than D) size distribution, as deduced from the magnitude data; its calibration is affected by the uncertainty in several parameters, including the reflection coefficient of the surface for sunlight (the geometric albedo). Mean values are assumed. A theoretical model (dashed line for the initial state, solid line for the evolved population) is also indicated. Data kindly provided by D. Durda and W.F. Bottke; see also D. Durda et al., *Icarus* **135**, 431 (1998).

one, Ceres, is about 950 km across. There are about 30 larger than 200 km, 250 larger than 100 km, 700 larger than 50 km. At smaller diameters D the size distribution becomes less known (current observations and models indicate there might be some 0.7 to 1 million asteroids larger than one km in the whole belt). The incremental main belt population is usually represented by a power law (Fig. 14.6)

$$dN \propto m^{-\alpha}\, dm \propto D^{\beta}\, dD \quad (\beta = 2 - 3\alpha)\ . \tag{14.2}$$

The observed value of α ranges from 1.3 to 2.0, implying that most of the asteroid mass lies in the largest bodies. The total mass is 2 or 3 times the one of Ceres, determined to be $1.56 \times 10^{-4}\, M_\oplus$ from the gravitational deflection of nearby objects. Variations of α in different size intervals likely reflect sinks of the small-object populations by non-gravitational effects and their fragility against impact disruption. With respect to an exact power law there is an excess of bodies with $D \approx 100$ km; this may be related to the fact that at this size the

self-gravitational binding energy, by re-accumulating the fragments ejected at speeds lower than the escape velocity into a "rubble pile" (Sec. 14.8), becomes important in determining the outcome of a disruptive impact. The distribution (14.2), with $\alpha \simeq 1.8$, has also been observed in fragments produced in laboratory impact experiments. However, asteroidal collisions involve sizes and energies which are typically 10^6 and 10^{18} times larger than those studied in the laboratory; scaling up outcomes of collisions by so many orders of magnitude is not straightforward. In the disruption of a laboratory object, part of the energy is necessary to overcome the tensile strength and to heat the body, while the rest goes to the kinetic energy of the ejecta; in asteroids, especially for events that lead to the formation of families, gravity confinement starts to play a dominant role. As we know today, the transition between the strength to the gravity regimes occurs at ≈ 200 m size. Escaping ejecta might also enter into bound orbits, sometimes resulting in the formation of binary objects. For these reasons, collisions between asteroid-size objects is far more complicated than laboratory experiments. Observational data of families and numerical models indicate for large sizes (≥ 10 km) a very steep distribution with $\alpha \simeq 2.1$, which at small sizes becomes shallower, with $\alpha \simeq 1.4$ – basically identical to that of the background population; this is probably due to collisional grinding. The observed size distribution of NEOs in the $1 - 10$ km size range is little steeper (with $\alpha \simeq 1.58$) than the corresponding population of the main belt, possibly due to size-selective transport processes, such as the Yarkovsky effect.

Rotation rates and their relation to asteroid structure. Most data about the rotation and the shape of asteroids come from light-curve photometry, which has provided rotational periods for $\approx 1,000$ bodies, and polar directions for ≈ 100 asteroids (Fig. 14.7). The median rotation period is about ≈ 10 hours for large-size asteroids ($\gtrsim 20$ km), and gets smaller for smaller sizes; but a large dispersion is present, and periods as short as 2.1 hours and as long as weeks have been observed. The correlations between spin period and taxonomic class is not yet understood, but a dependence on the mean density has been suggested (in the average C-type and M-type asteroids rotate, respectively, slower and faster). Since the asteroid angular momenta have been affected in a complex way by, and to a large degree acquired in, collisional and dynamical processes, rotation states certainly are not primordial.

Apart from the "normally" rotating population, we have two extreme subpopulations (Fig. 14.7): (i) *slow rotators*, with periods typically larger than a day, the slowest at ≈ 47 d; and (ii) *fast rotators*, with periods less than ≈ 2.1 h. This limit derives from condition $\omega_{\rm cr}^2 \simeq \frac{8}{3}\pi G\,\bar{\varrho}$, which sets the largest angular velocity $\omega_{\rm cr}$ for a homogeneous body of density $\bar{\varrho} \simeq 2.5$ g/cm^3 and vanishing strength against rotational fission. Interestingly, this limit is clearly seen in the small-asteroid rotation data down to sizes of ≈ 150 m (Fig. 14.7), supporting the idea that they have fractured and low-strength internal structures.

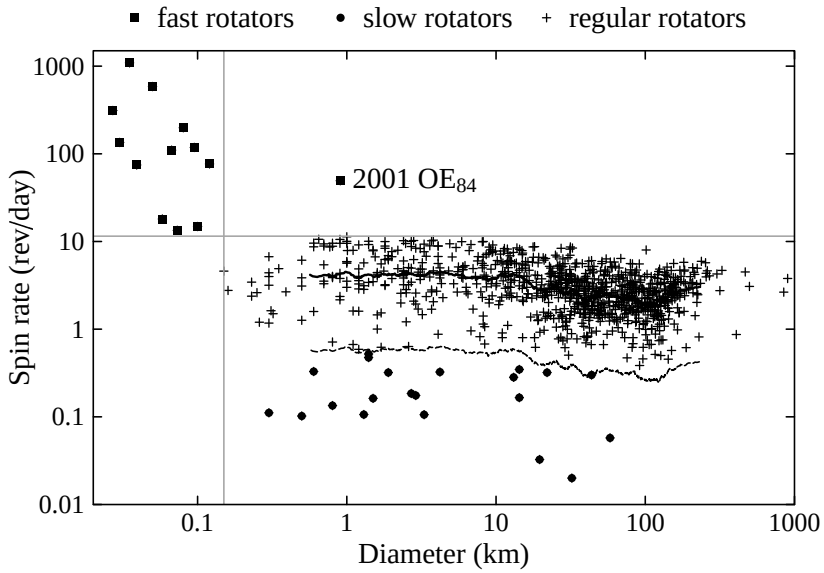

Figure 14.7. Asteroids in the (diameter, spin rate) plane, in logarithmic units. The thick line shows the average spin rate for objects larger than 1 km. The shallow minimum at $\simeq$ 100 km corresponds to the "angular momentum drain" process: when the velocities of the fragments from an impact are near the escape velocity, more objects escape in the prograde sense relative to the rotation of the asteroid, and with their recoil slow down the spin. Full circles below the dashed line, at three standard deviations from the mean, are slow rotators, with unusually long periods, up to a few months. Full squares on the upper left are fast rotators – small near-Earth asteroids with periods as short as a few minutes. The horizontal line at $\simeq$ 12 rev/day, a population boundary above the size of $\simeq$ 150 m, is due to the disruption of loosely bound, faster objects by the centrifugal force; a single exception is the recently discovered 2001 OE_{84}, with a rotation period of 29.19 min and a size of about 900 m. Note that in the population of small bodies, all the near-Earth asteroids observable during a very short window of time, there is a large observational bias toward short periods. Data for nearly 1,000 asteroids kindly provided by P. Pravec.

Only objects with small sizes, which likely are monolithic, can rotate faster. The sub-population of slow rotators is still unexplained; one viable scenario assumes that asteroids undergo braking due to a loss of a close satellite. At smaller sizes, radiation torques may also despin the body (Problem 15.10).

The accidental discovery by the Galileo spacecraft in 1993 of Dactyl, a small satellite orbiting about the asteroid Ida, opened the investigation of *binary asteroids*. In mid 2002 10 more binary systems in the main belt were known, including one satellite of a Trojan asteroid. These pairs were discovered with very high resolution techniques using adaptive optics and large optical telescopes (including the Hubble Space Telescope). 13 more binary systems were found in the NEO population by optical and radar observations. The orbital

motion of binary asteroids yields valuable information about their mass and mean density, typically difficult to access. Current estimates suggest a fraction of a few % of binary systems among the main belt asteroids, but up to 20% among NEOs. The ratio of sizes of the two components ranges between 0.01 and 1, from a primary with a small satellite to a truly double system. The NEO binary systems are characterized by a small separation (not exceeding 10 times the radius of primary) and a small eccentricity of the relative motion (≤ 0.1); there is also indication that the primary always has a short rotation period in the $2 - 3$ h range. The origin of binary asteroids, as well as their long-term dynamical stability, is not well known. Some of them might be ejecta that, under favourable conditions, formed during collision of a parent body (as during family formation); another possibility is a capture of ejecta in a non-disruptive cratering event on the primary. In the case of NEOs there might be more possibilities: tidal fission due to close encounter with a planet or rotational fission due to the YORP effect (see Problem 15.10).

Chemical composition of asteroids. In the last few decades an intense observational effort has shed light on the problem of asteroid composition, which has been found to be very diverse. The main source of information is spectral analysis of reflected sunlight, but other techniques, like infrared observations, polarimetry and planetary radar, have been applied as well. These data have then been interpreted by comparing them with the properties of minerals found in different meteorite types.

A clear difference among various types of surfaces is found in the distribution of albedo. When observational biases against darker objects are accounted for, some 75% of the asteroids are found to be very dark, with average $A \approx 0.04$. A distinct group of bodies have a moderate albedo of about 0.15, with few asteroids lying in between and a tail of "bright" bodies with A up to 0.4 and more. A better discrimination is possible if spectrophotometry data are used, yielding the behaviour of the reflection spectrum over a wide wavelength interval (Fig. 14.8). Some absorption bands are unequivocal evidence of silicates, water ice and hydrated minerals, but in many cases these prominent features are lacking, and any inference about the mineral composition must be regarded as conjectural.

Statistical clustering techniques have been applied to sets of observational parameters, potentially relevant for the surface composition of asteroids, in order to define the so called *taxonomic types*. C-type asteroids have a very low albedo and a flat spectrum throughout the visible and the near infrared; they are probably similar in composition to carbonaceous chondritic meteorites, which are primitive mineral assemblages subjected to little, or no, metamorphism after their condensation. D-type objects are also dark, but have very red spectra, suggesting the presence of low-temperature organic compounds. These objects are similar to many low-albedo, reddish small bodies found in the outer

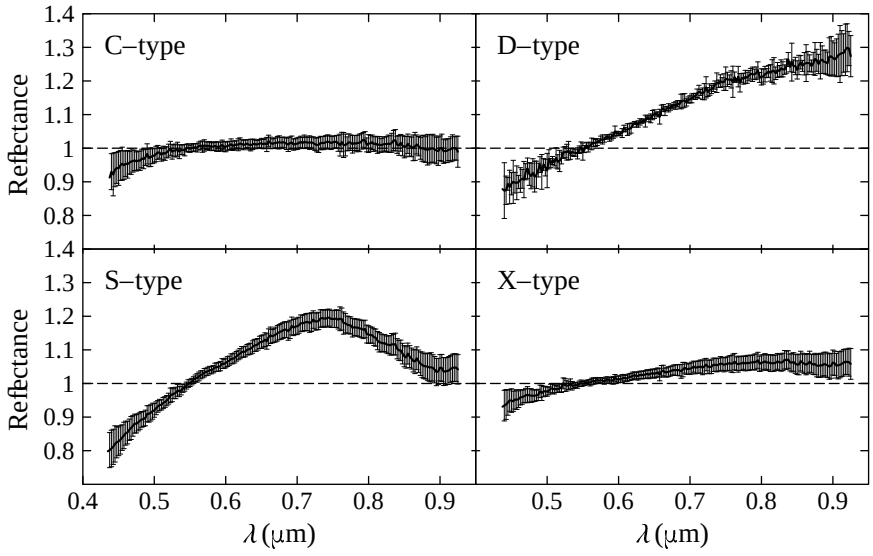

Figure 14.8. Mean optical reflectance spectra of asteroids of the taxonomic classes C, D, S and X; mean values over the whole sample of known asteroids of the corresponding class are shown; the spectral reflectance is normalized to unity at 0.55 μm. Note the absorption near 0.9 μm in the S-class, an evidence for silicates on the surface. Data from http://smass.mit.edu/.

solar system, including some comets observed at low activity and a few small satellites (e.g., Phoebe). S-type asteroids have a relatively high albedo, and their spectra show absorption bands due to silicates, like pyroxene and olivine (Fig. 14.8). It is debated whether they are analogous to stony-iron meteorites (probably derived from core-mantle interfaces of differentiated parent bodies), or ordinary chondrites, interpreted as assemblages of primitive nebular grains of different compositions, subsequently moderately heated and metamorphosed. If surface alteration by energetic solar radiation, cosmic rays and micrometeorite impacts (generally called *space weathering*) is taken into account, the analogy with ordinary chondrites appears likely; in particular, spectral analysis of S-type NEOs allowed to establish a link between these objects and the ordinary chondrites meteorite class. M-type asteroids have an albedo of about 0.1, with slightly reddish spectra, suggesting a significant content of nickel-iron alloy (this interpretation has been confirmed by radar observations; in the modern classification system this group is part of the X-type class). It is likely that they are akin to iron meteorites, and hence represent pieces of cores of differentiated precursors.

Of great interest is the fact that different taxonomic types are, on average, preferentially located at different heliocentric distances. This orderly progression is usually interpreted as reflecting both variations in the composition of

the material which condensed in the solar nebula, due to the decrease in temperature with solar distance, and the different relevance of subsequent melting events and metamorphism. Indeed, the most primitive types (C and D, corresponding to least metamorphosed material) tend to lie in the outer belt, where most asteroids significantly resemble cometary nuclei. However, the borders between the radial location of asteroids with different spectral properties are not sharp, and overlap by a fraction of AU. This feature likely originates in the early violent perturbation of the asteroid belt by massive planetesimals.

14.4 Transneptunian objects and Centaurs

The discovery in the 1990s of a population of objects beyond Neptune, named *transneptunian objects* (TNOs), was a major event in planetary science, on a par with the discovery of the solar wind and planetary magnetospheres earlier in the 20th century. For the first time after 1801, when the first asteroid was observed by G. PIAZZI, an entirely new class of objects in the solar system was discovered. The prediction on theoretical grounds of Kuiper belt objects before their discovery strengthens its importance.

From the historical viewpoint, the theoretical arguments were basically two. First, as mentioned in Sec. 14.1, Pluto has always appeared an oddity among planets and it was also not clear why accretional formation of the solar system objects should stop at Neptune's distance (with the exception of the tiny Pluto). This was the original motivation which led G.P. KUIPER, and, independently, K.E. EDGEWORTH, in the 1940s and 1950s to expect a disc of objects in the transneptunian region. A more immediate motivation came from study of the Jupiter family comets (Sec. 14.5). This numerous population is characterized by low inclinations and there is no known physical mechanism that could confine their orbits to the invariable plane of the solar system when the source is far away and isotropic (like the Oort cloud; Sec. 14.5). For that reason, theorists in the 1980s postulated a disc of cometary objects beyond Neptune that could act as a source for short-period comets.

The turning point was discovery of 1992 QB_1, the first transneptunian body (apart from Pluto and its satellite Charon). Since that time some $\approx$ 800 more members of this population have been observed, with an accelerating rate of discovery in the past few years. So far the largest known members of the TNO population are about 900 km across (there are about 4 objects with this size, including 2000 WR_{106}, named Varuna). This is about the same size as Ceres, the largest asteroid. Their number rapidly increases with diminishing size, with an estimate of $\approx 40,000$ objects larger than 100 km. The smallest observed TNOs have a size of about 25 km, but little is known about bodies below $\approx$ 50 km. Pluto is also not alone to have a satellite among the TNO population. Seven more TNOs possess a companion; the best known system,